APMIS JOURNAL OF PATHOLOGY, MICROBIOLOGY AND IMMUNOLOGY

APMIS 131: 381–393

DOI 10.1111/apm.13306

Multiple myeloma cell-derived exosomes promote favorable tumor functional performance by polarizing macrophages toward M2-like cells

BAHMAN RAZI,[1] MASOUD SOLEIMANI,[1,2] MINA SOUFI-ZOMORROD,[3] AHMAD ADELI[4] and NOUSHIN DAVOUDI[4]

[1]Department of Hematology, Faculty of Medical Sciences, Tarbiat Modares University; [2]Department of Tissue Engineering and Applied Cell Sciences, School of Advanced Technologies in Medicine, Shahid Beheshti University of Medical Sciences; [3]Department of Hematology Applied Cell Sciences, Faculty of Medical Sciences, Tarbiat Modares University; and [4]Biotechnology Research Center, Pasteur Institute of Iran, Tehran, Iran

Razi B, Soleimani M, Soufi-Zomorrod M, Adeli A, Davoudi N. Multiple myeloma cell-derived exosomes promote favorable tumor functional performance by polarizing macrophages toward M2-like cells. APMIS. 2023; 131: 381–393.

It has long been hypothesized that leukemic cells are able to modulate the fate of resident cells in the tumor microenvironment (TME) toward either supporting or immunosuppressive cells for the development of tumors. Exosomes can be a potential culprit in imposing tumor desire. There is evidence about the impact of tumor-derived exosomes on different immune cells in different malignancies. However, findings about macrophages are contradictory. Here, we evaluated the potential influence of multiple myeloma (MM)-cell-derived exosomes on the polarization of macrophages by examining hallmarks of M1 and M2 macrophages. After treatment of M0 macrophages with isolated exosomes (from U266B1), gene expression (Arg-1, IL-10, TNF-α and IL-6), immunophenotyping markers (CD206), cytokine secretion (IL-10 and IL-6), nitric oxide (NO) production, and redox potentiality of target cells were assessed. Our results revealed significantly increased expression of the genes involved in the development of M2-like cells but not M1 cells. The CD 206 marker and IL-10 protein levels were significantly increased at different time points. The expression of IL-6 mRNA and IL-6 protein secretion did not change significantly. MM-cell-derived exosomes induced significant changes in NO production and intracellular ROS levels in M0 cells.

Key words: Exosome; macrophage polarization; multiple myeloma.

Masoud Soleimani, Department of Hematology Applied Cell Sciences, Faculty of Medical Sciences, Tarbiat Modares University, 14115-331 Tehran, Iran. e-mails: soleimani.masoud@gmail.com; soleim_m@modares.ac.ir

Multiple myeloma is an incurable lymphoproliferative disease of B lymphocyte origin [1,2]. It is manifested by high-speed growth of monoclonal plasma cells that leads to mass production of malfunction immunoglobulin (Ig) chains. Accumulation of these abnormal immunoglobulins and monoclonal plasma cells in bone marrow (BM) results in major pathologic symptoms, including anemia, bone lesions, infection, and renal dysfunction [1,3]. From an epidemiological perspective, MM accounts for 1% of all cancers worldwide and is the second most prevalent hematologic malignancy [4]. Age over 60 years, positive family history, male sex, and black race are favorable risk factors for a high incidence of MM [5,6]. The key points in understanding MM pathophysiology come from the communication between myeloma cells and the BM microenvironment components that results in the progression of malignancy [7]. More specifically, myeloma cells trigger reprogramming of normal resident cells of the BM toward malignant tumor-supporting cells. This process is managed by extracellular vesicles (EVs) communicated between myeloma cells and BM resident cells.

Extracellular vesicles are a group of secretory vesicles that include three subpopulations: exosomes,

Received 13 February 2023. Accepted 28 February 2023

microvesicles/shedding particles, and apoptotic bodies [8]. In recent years, numerous studies have focused on exosomes as new actors in the crosstalk between cancer cells and normal cells in the TME. These nanoparticles share several characteristics in common, including size (50–150 nm), specific markers (CD9, CD63, CD81, etc.) and ability to affect their surrounding microenvironment or distant tissues. Exosome content reflects the molecular characteristics of their parent cells and contains a wide variety of membrane and cytoplasmic proteins, including receptors, lipids, enzymes, nucleic acids (mtDNA, ssDNA, dsDNA, mRNA and miRNA), and transcription factors [9–11].

Exosomes derived from malignant cells create a supportive microenvironment by reprogramming BM resident cells, including immune cells, mesenchymal stem cells (MSCs), endothelial cells, etc., which culminates in immune suppression, tumor progression and evasion [12,13]. Several clinical studies have confirmed the pathologic function of exosomes. Accordingly, both the monoclonal immunoglobulin free light chain [14] and the monoclonal immunoglobulin of the B-cell receptor have been demonstrated on MM-cell-derived exosomes [15]. When examining plasma cell markers, it was found that CD138 was more highly expressed in MM cell-derived exosomes than in healthy controls, correlating with the therapeutic response and disease stage [16,17]. Additionally, in a follow-up study, the multidrug resistance protein P-glycoprotein, together with the stem cell marker CD34 on CD138− exosomes in patients with MM, correlated with unresponsiveness to treatment.

Among immune cells, resident macrophages are one of the most important immunoregulatory cells, causing fundamental changes in the TME in favor of tumor cells [18]. In response to tumor-derived signals (such as exosomes), macrophages undergo phenotypic polarization toward a supportive cell for the tumoral microenvironment. Commonly, macrophages are able to polarize toward M1 (classically activated) and M2 (alternatively activated) phenotypes, both of which can affect tumor-related inflammatory status [19,20]. M1 macrophages (characterized by iNOS, ROS, TNF-α), which are tagged as tumor-resistant cells. Unlike M1 macrophages, M2 cells have the potential to act as immune suppressors in the tumor nest. M2 cells (characterized by IL-10, Arg-1, CD206hi) are prone to promote stromal activation, angiogenesis, and remodeling, thereby augmenting cancer progression and the poor prognosis of cancerous patients [21].

In contrast to these theoretical facts, the results of some studies have shown the possibility of macrophage polarization to the M1 phenotype in the tumoral microenvironment. Xiao *et al*. indicated that THP-1-derived macrophages exhibited an M1-like phenotype when treated with exosomes derived from the oral squamous cell carcinoma (OSCC) cell line [22]. Furthermore, Shao *et al*. labeled SW620-EVs with PKH26 and cocultured them with the RAW264.7 (mouse) and THP-1 (human) macrophage cell lines. While Arg-1 and IL-10 mRNA levels did not change, TNF-α mRNA was significantly increased in macrophages treated with CRC-EVs, mirroring M1 phenotype development subsequent to incubation with tumor-derived EVs [23].

The mentioned studies highlighted that macrophage polarization might depend on the type of malignancy. Previously, studies examined the influence of exosomes on different residents of the TME, and studies on macrophages were contradictory. Here, for the first time, we investigated the influence of MM cell-derived exosomes on the polarization of the THP-1 cell line toward macrophage phenotypes. Moreover, we tried to examine all hallmarks for both the M1 and M2 phenotypes. The findings of this study will hopefully pave the way toward future studies to investigate the molecular pathways and mechanisms involved in the polarization of macrophages by MM cell-derived exosomes as well as to contemplate clues for clinical studies.

MATERIALS AND METHODS

Cell culture

The U266 and THP-1 cell lines were purchased from the Pasteur Institute of Iran. Both cell lines were cultured in growth medium containing RPMI 1640 supplemented with 10% fetal bovine serum (FBS) (DNA BioTech, Tehran, Iran), 1% penicillin–streptomycin (Gibco, Norristown, PA, USA), and 2 mM L-glutamine (at 37 °C in a humidified 5% CO2 atmosphere). Human monocytic THP-1 cells were differentiated into resting macrophages (M0) by 24 h incubation with 50 ng/mL PMA (Sigma–Aldrich, Saint Louis, MO, USA) followed by 24 h rest in fresh RPMI 1640 medium [24,25]. Anti-CD11b-FITC (Bio Legend, San Diego, CA, USA), along with the corresponding isotype controls, was used to confirm the differentiation of THP-1 cells into macrophages. Moreover, granule density and cytoplasmic changes in resting macrophages in comparison with monocytic THP-1 cells were examined by flow cytometry analysis. FBS contains large numbers of bovine EVs, which hampers the analyses of secreted EVs from the cell type of preference and the downstream analyses. Therefore, FBS was depleted from EVs by an ultrafiltration-based protocol described by Kornilov *et al*. [26] with some modifications. Since FBS is a viscose and concentrated liquid, it might block Amicon Ultra-15 Centrifugal Filter Units (MWCO: 100 kDa; Merck Millipore, Burlington, MA, USA). To solve this issue, RPMI 1640 medium supplemented with 10% FBS was ultrafiltered for 55 min at 3000 *g*. The liquid that passed through the filter was denoted exosome-depleted FBS. It is obvious that

alongside exosomes, many other nutritious ingredients were also extracted from FBS. Therefore, cell culture adaptation with exosome-depleted FBS is necessary.

Cell adaptation and exosome isolation

The U266B1 cell line was cultured in RPMI 1640 medium supplemented with 10% FBS. To adapt the MM cell line with exosome-depleted FBS, a 10-day culture was applied. The adaptation process was started with cells in the logarithmic growth phase at a cell density of 5 × 105 cells/mL cultured in a T25 flask (cell viability > 95%). Then, the mixture was transferred to a T75 flask. Every other day, we added 5 mL medium (4 mL RPMI1640 with usual FBS and 1 mL RPMI1640 with exosome-depleted FBS on the third day, the usual FBS gradually decreased and ultrafiltered FBS increased). On the tenth day, we added RPMI 1640 with exosome-depleted FBS. When the cells were completely stabilized in RPMI 1640 medium supplemented with 10% exosome-depleted FBS, the adapted cells were cultured, and subsequently, conditioned media (CM) was removed for exosome isolation. CM was subjected to serial centrifugation, according to Lobb *et al*. [27] with some modifications: 10 min at 300× *g* for removing live cells, filtered through 0.22 μm filters to remove apoptotic bodies, macro vesicles and cell debris, and finally, 90 min ultracentrifugation at 100 000 *g* avg at 4 °C to pellet exosomes. The pellets were resuspended in phosphate-buffered saline (PBS) and utilized for all *in vitro* experiments.

Exosome quantification by BCA assay

To quantify the amount of isolated exosomes, aliquots (20 μL) of isolated exosomes were dispensed into wells of a 96-well plate, and their protein content was measured using a bicinchoninic acid assay (BCA) protein assay kit (DNA BioTech, Tehran, Iran) according to the manufacturer's instructions. Total protein concentrations were determined using a linear standard curve established with BSA.

Western blotting

To characterize and confirm the presence of isolated exosomes, immunoblotting was applied for CD9 and calnexin, which are markers of exosomes. Briefly, cell lysates were extracted using RIPA buffer, and the content of each sample was determined by a BCA protein assay kit. First, 20 μg of denatured protein samples were loaded onto 12% (v/v) sodium dodecyl sulfate-polyacrylamide gel electrophoresis (SDS-PAGE), and the results of electrophoresis were transferred to a polyvinylidene fluoride (PVDF) membrane. In the next step, the membranes were blocked using 5% skimmed milk for 1 h. The blots were stained with a specific primary antibody (Sino Biological Inc. Beijing, China) and incubated overnight at 4 °C. Then, the membranes were washed 3 times with TBST and incubated with mouse HRP-conjugated secondary antibody for 1 h. Finally, the protein expression level was detected by ECL Western blot analysis substrate.

Transmission electron microscopy

To determine the specifications of exosomes by transmission electron microscopy (TEM), 20 μL of isolated exosomes was first resuspended and pipetted onto a carbon film 300 mesh cooper grid (AGS160–3) and dried within 5 min. Then, it was stained with drops of 1% uranyl acetate at room temperature (RT). Eventually, the carbon film was air-dried for imaging analysis. A Zeiss-EM10C transmission electron microscope (Carl Zeiss, Jena, Germany) was used to image the prepared samples at a voltage of 80 kV.

Scanning electron microscopy

An overview of the isolated exosomes was observed using SEM. Accordingly, 20 μL of isolated exosomes was resuspended and deposited on aluminum foil (5 min) and fixed with 4% paraformaldehyde at RT. The fixed exosome was dehydrated with an ascending sequence of ethanol (50%, 70%, 80%, 90%, and 100% absolute ethanol). The sample was air-dried at RT and then analyzed by SEM (KYKY-EM3000, 30 kV, China).

Size measurement of exosomes by dynamic light scatter

The size distribution of isolated exosomes was determined by DLS Nanotrac Wave II (Microtrac Inc, Osaka, Japan). Briefly, the volume of isolated exosomes was brought to 1 mL with PBS and loaded into a quartz cuvette. Then, we measured the size distribution of exosomes at 25 °C.

Cell viability (MTT assay)

THP-1 monocytes (10^4 cells/well) were seeded in 96-well plates and differentiated into macrophages as described previously. After incubation with different exosome concentrations (25, 50, 75, and 100 μg) at different time points (24, 48, and 72 h), the cells were incubated for 3 h with 10 μL of MTT reagent in a CO2 incubator. The 96-well plates were centrifuged at 300 × *g* for 5 min, the medium was removed, and 100 μL of DMSO was added to each well. Plates were first gently shaken at 618 *g* for 20 min, and the absorbance was measured by an ELISA reader at 570 nm.

Internalization assay

To detect exosomes and check their fusion with the target cells, exosomes were first labeled with CFSE (Invitrogen, Waltham, MA, USA) by incubating at 4 °C for 10 min. Then, exosomes were added to resting macrophage culture media, and after incubation in a humidified CO_2 incubator, the cells were fixed and stained with DAPI for nuclear staining. A CYTATION imaging reader (Biotek, Winooski, VT, USA) was used for further analysis.

Nitric oxide measurement

The level of NO measured from the existence of nitrite (NO_2^-) as a stable metabolite of nitric oxide in the culture supernatants of exosome-treated M0 using the Griess reaction. Accordingly, 100 μL of Griess reagent containing 1% sulfanilamide and 0.1% naphthylenediamine in 5% phosphoric acid (Merk, Germany, Darmstadt) was added

to 100 μL of each culture supernatant sample and incubated at RT for 10 min. The optical density (OD) of the samples was immediately measured at 540 nm on an ELX800TM plate reader (BioTek, Winooski, VT, USA).

Determination of intracellular reactive oxygen species

Intracellular ROS production in exosome-treated M0 cells was determined using 2,7-dichlorodihydrofluorescein diacetate (H2DCFDA; Sigma–Aldrich, Saint Louis, MO, USA). The exosome-treated cells were collected and washed with PBS at different time points. Then, 500 μL of dye solution containing 10 μM H2DCFDA was added to each sample, and the cells were maintained in a dark and humidified 37 °C condition for 45 min. After the incubation period, the cells were centrifuged and again washed with PBS and evaluated by flow cytometry for ROS production (BD, FACS Canto II, BD Bioscience, Franklin Lakes, NJ, USA). The results were analyzed using FlowJo software version 2-1.

RNA extraction, cDNA synthesis and qRT-PCR assay

To determine the mRNA expression levels of target genes, THP-1 cells were first seeded in 6-well culture plates, and after differentiation into macrophages (M0), they were treated with 50 μg/mL isolated exosomes for 24, 48, and 72 h. Total RNA was extracted using TRIzol Reagent (Invitrogen, Carlsbad, CA, USA). A NanoDrop 8000 (Thermo Scientific, Waltham, MA, USA) was used to detect the concentration and purity of RNA samples in 260/280 nm and 260/230 nm ratios, respectively. Finally, total RNA was dissolved in 20 μL DEPC water. Complementary DNA (cDNA) was synthesized with an Easy cDNA Synthesis Kit according to the manufacturer's instructions (Parstous, Tehran, Iran). Real-time PCR using SYBR Green Master Mix (©Ampliqon, Herlev, Denmark) was accomplished in a 0.1 mL tube and run in a Step One Real-Time PCR System Applied Biosystems (Waltham, MA, USA). Fold changes in the expression of selected genes between the control and exosome-treated groups were analyzed using the $2^{-\Delta\Delta CT}$ method. β-Actin was used as a housekeeping gene. The primer sets used for qRT–PCR are listed in Table 1.

Cytokine assay

The supernatant of the exosome-treated/PBS-treated cells was centrifuged at 1200 rpm for10 min at 4 °C to remove debris. Subsequently, the concentrations of IL-6 and IL-10 cytokines were evaluated by ELISA kits (BD Biosciences, Franklin Lakes, NJ, USA) according to the manufacturer's protocol. Finally, the OD was measured at 450 nm by an ELX800TM plate reader (Biotek, Winooski, USA).

Table 1. The primer sequence used in qRT-PCR test

Gene	Sequence
Arg-1	F5′-TGGACAGACTAGGAATTGGCA-3′
	R5′-CCAGTCCGTCAACATCAAAACT-3′
IL-10	F5′-ATGAGCATTCAGACTGGGTAAAC-3′
	R5′-TTTTAGGGGCTAAGAAACGCAT-3′
TNF-α	F5′-TCCCCAGGGACCTCTCTCTA-3′
	R5′-GAGGGTTTGCTACAACATGGG-3′
IL-6	F5′-TCAATGAGGAGACTTGCCTG-3′
	R5′-GTCAGGGGTGGTTATTGCAT-3′
β-Actine	F5′-TGAAGATCAAGATCATTGCTCCC-3′
	R5′-AGTCATAGTCCGCCTAGAAGC-3′

Statistical analysis

Data are represented as the mean ± SEM. The Mann–Whitney U test or one-way ANOVA was used to make comparisons between different groups. GraphPad Prism 6.07 software was used for analysis. The statistical significance threshold was set as $p < 0.05$.

RESULTS

THP-1 cell differentiation into M0 macrophages

To confirm the acquisition of a macrophage-like phenotype, hallmarks of macrophages, including adhesion and increased cytoplasmic volume, spreading morphology, and enhanced granularity, were evaluated. In this regard, Giemsa staining was used to clearly display morphological differences between differentiated and undifferentiated THP-1 cells by phase-contrast microscopy (Fig. 1B). Furthermore, movement in the direction of the side scatter (SSC) axis on flow cytometry figures revealed granularity enhancement (Fig. 1C). The other remarkable parameter that confirms the differentiation of THP-1 cells is alterations in cell surface markers. As shown in Fig. 1D, incubation of THP-1 cells with PMA induced differentiation to adherent CD11b-positive macrophages referred to as M0 [28].

Characterization of U266B1cell line-derived exosomes

Transmission electron microscopy and SEM indicated morphologically round and disc-shaped exosomes (Fig. 2A,B). The average size of exosomes was between 50 and 150 nm. According to the Zetasizer results, the average size was 124.7 nm (Fig. 2C). Western blotting analysis demonstrated the presence of the exosome-specific markers CD9 and calnexin in the exosome pool and control (Fig. 2D). Taken together, the morphology, size, and specific marker results confirmed the presence of exosomes.

Assessment of exosome uptake by M0 macrophages

Fluorescent labeling of exosomes *via* CFSE dye was applied to assess the potential of M0 cells to take up labeled exosomes. After the preparation period, M0 macrophages had the capacity to incorporate and localize to the cytoplasm of isolated exosomes (Fig. 2E).

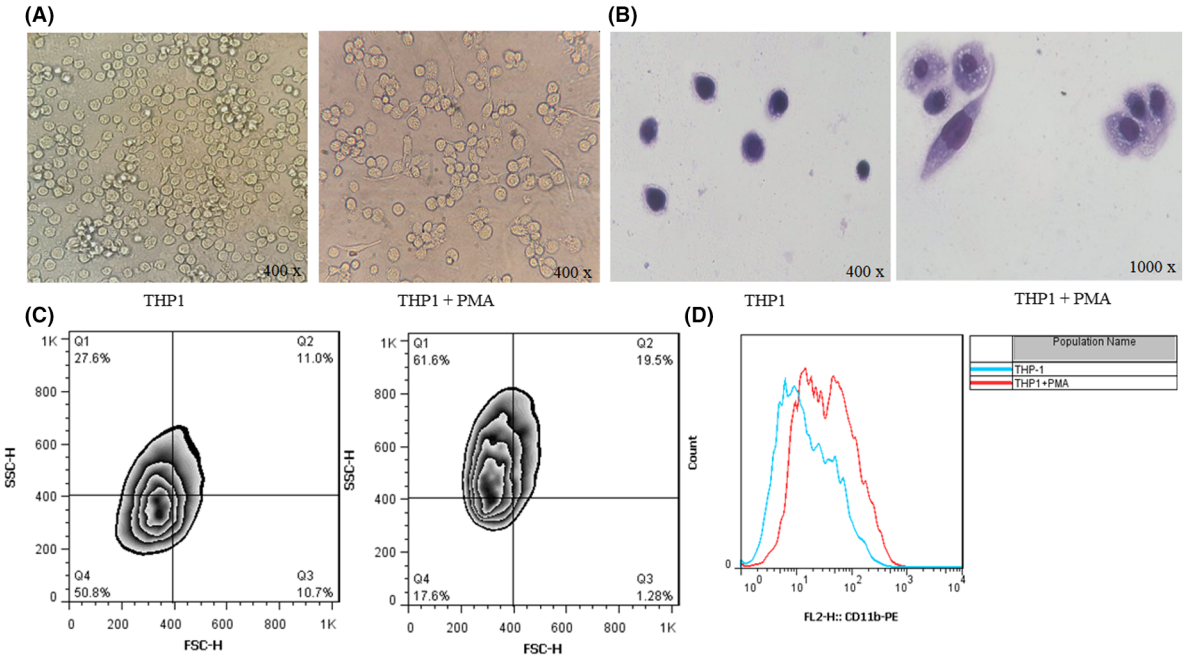

Fig. 1. Monocytic THP-1 differentiation into resting macrophages (M0): (A) Morphological analysis of THP-1 cells (left side) and THP-1 cells +PMA after 48 h (24 h culture in RPMI1640 + PMA and 24 h resting in fresh RPMI1640 without PMA). (B) THP-1 cells stained with Giemsa stain (left side), THP-1 cells +PMA after 48 h (24 h culture in RPMI1640 + PMA and 24 h resting in fresh RPMI1640 without PMA) stained with Giemsa stain that clearly show spread cytoplasm, larger nucleus and cytoplasmic granules. (C) Flow cytometric analysis of side scatter changes. (D) Surface marker expression (CD11b) in the differentiation of THP-1 cells to macrophages (M0).

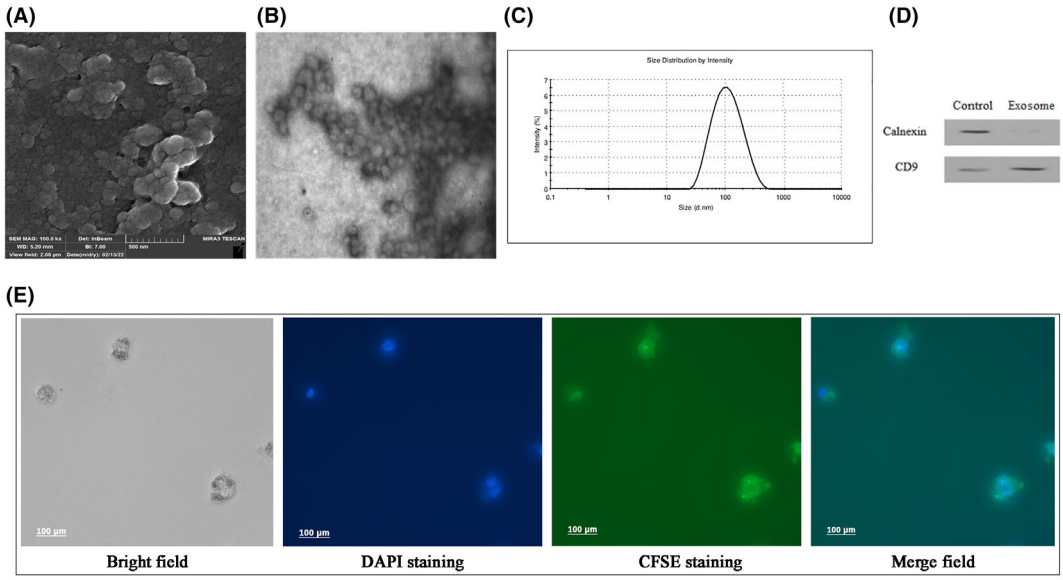

Fig. 2. Characterization and uptake of U266-derived exosomes: (A) Scanning electron microscopy image of U266-derived exosomes. (B) Transmission electron microscopy image of U266-derived exosomes. (C) Size analysis of U266-derived exosomes using dynamic light scattering. (D) Western blotting analysis indicates the presence of CD9 protein in U266-derived exosomes and calnexin in cell lysates. (E) Florescent microscopy with a CYTATION image reader confirmed uptake and internalization of U266-derived exosomes (labeled with the CFSE lipophilic dye) by recipient cells with their nuclei stained by DAPI.

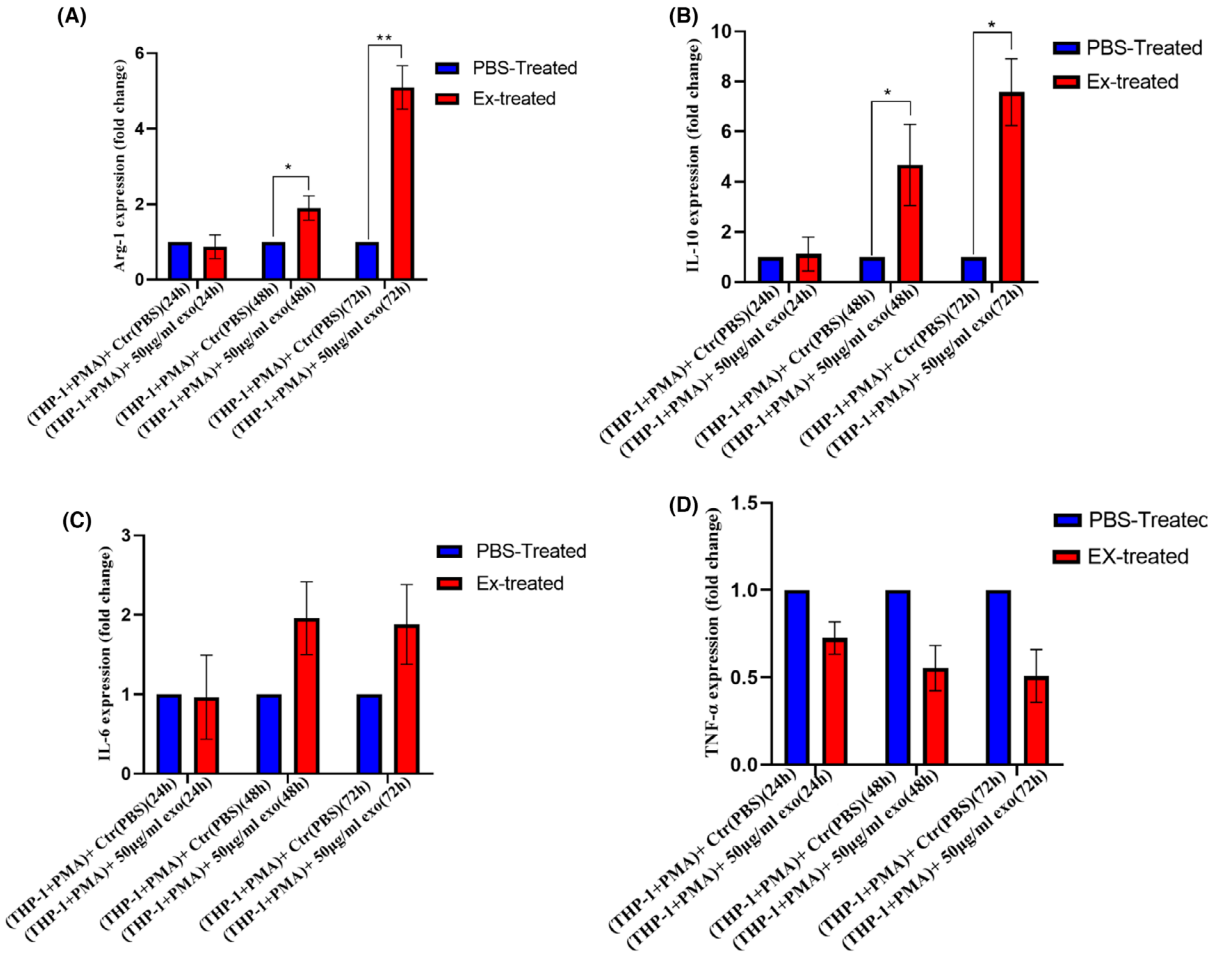

Fig. 3. Gene expression level in resting macrophages after treatment with U266-derived exosomes at 24, 48, and 72 h time points. (A) Arg-1 variation after exposure to exosomes. (B) IL-10 variation after exposure to exosomes. (C) IL-6 variation after exposure to exosomes. (D) TNF-α variation after exposure to exosomes. The data are representative of two independent experiments presented as the mean ± SEM. **p < 0.01, *p < 0.05.

U266B1 cell line-derived exosomes polarize M0 macrophages toward M2-like cells

Exosomes are a well-known microenvironmental stimulator that might change the fate of undifferentiated macrophages (M0) in favor of tumoral cells. To evaluate the potential polarization of resting macrophages toward the M2-like phenotype, the gene expression of Arg-1 and IL-10 was examined. The results confirmed significant expression levels of Arg-1 (0.44 ± 0.12, p = 0.05, and 0.49 ± 0.15, p = 0.009) and IL-10 (3.67 ± 1.14, p = 0.04, and 6.57 ± 0.94, p = 0.01) in M0 macrophages at 48 and 72 h after treatment with U266B1-derived exosomes (Fig. 3). Parallel with the qRT–PCR findings, the level of CD206 was increased after 48 (10.35 ± 0.52, p = 0.002) and 72 h (13.75 ± 0.55, p = 0.001) of treatment with isolated exosomes (Fig. 4). Finally, the ELISA results at 24 h did not reveal a significant change in IL-10 levels between the U266B1-derived exosome-treated group and the control group (1.82 ± 0.78, p = 0.14). However, IL-10 levels were higher in the supernatant of M0 cells treated with exosomes than in the control group at 48 h (17.64 ± 1.37, p = 0.006) and 72 h (27.02 ± 1.84, p = 0.004; Fig. 5). Based on the mentioned examination, we conclude that MM-dcell-erived exosomes change the performance and function of resting macrophages toward M2-like cells.

U266B1 cell line-derived exosomes do not induce hallmarks of M1 macrophages

Classical M1 macrophages secrete a large number of inflammatory genes and chemokines that

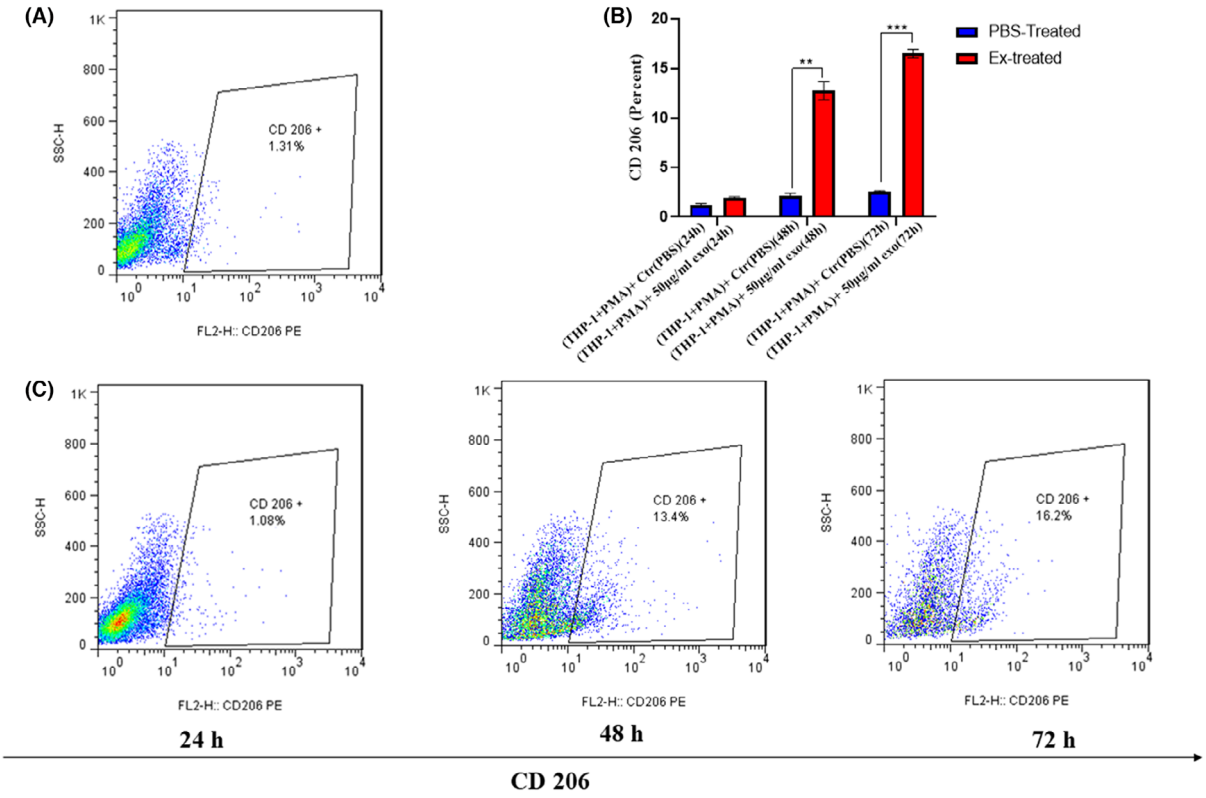

Fig. 4. Flow cytometric analysis of the CD206 marker in resting macrophages after treatment with U266-derived exosomes at 24, 48, and 72 h time points. The data are representative of two independent experiments presented as the mean ± SEM. **p < 0.01.

facilitate and promote antigen presentation to cytotoxic T cells in response to killing activity. The results of M0 macrophage treatment with 50 µg/mL MM-cell-derived exosomes did not significantly change the mRNA levels of TNF-α at 24 (0.27 ± 0.09, p = 0.09), 48 (0.44 ± 0.12, p = 0.75) and 72 h (0.49 ± 0.15, p = 0.08) in comparison with the control group (treated with PBS; Fig. 3).

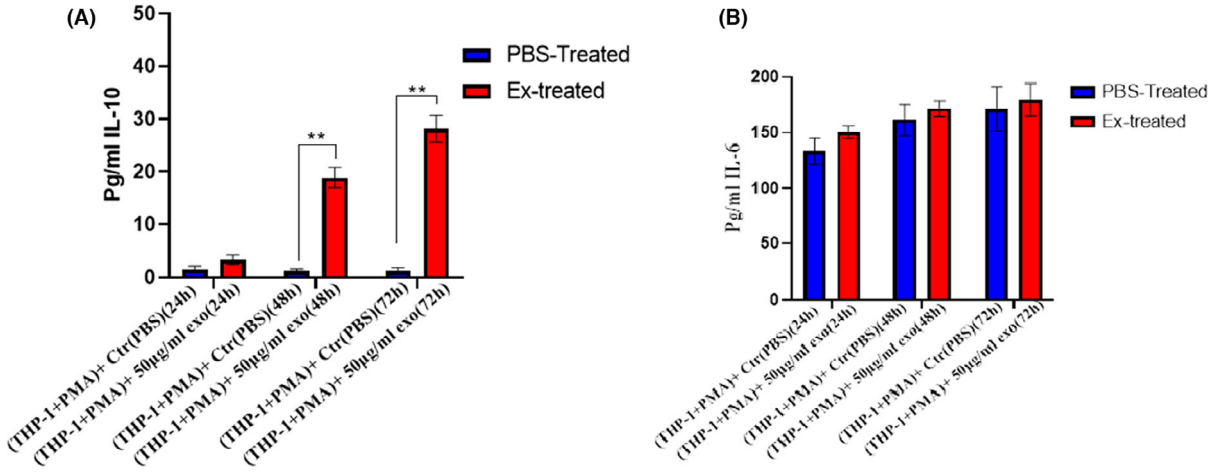

Fig. 5. Effect of U266-derived exosomes on the production of nitric oxide (NO) in the supernatant of resting macrophages treated with exosomes at 24, 48, and 72 h time points. The data are representative of two independent experiments presented as the mean ± SEM. **p < 0.01.

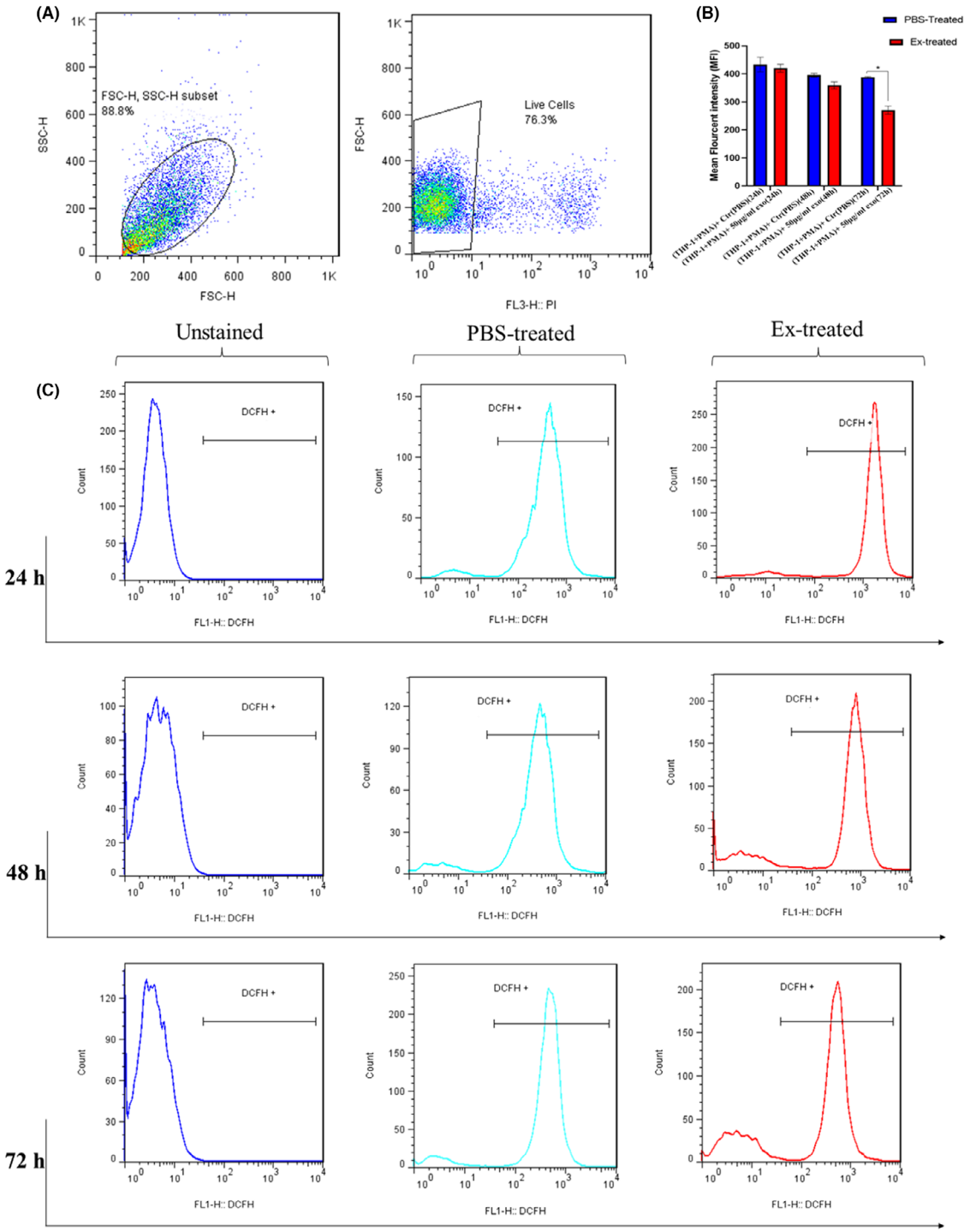

Fig. 6. Flow cytometric analysis of intracellular ROS generation in resting macrophages after treatment with U266-derived exosomes at 24, 48, and 72 h time points. (A) Graph represents the cell population by using an FSC-A versus SSC-A plot. (C) Histograms show the comparison of intracellular DCF fluorescence intensity in the unstained control group, control (PBS treated) group, and exosome-treated group. (B) Comparison of ROS levels between the control (PBS treated) and exosome-treated groups. The data are representative of two independent experiments presented as the mean ± SEM. *$p < 0.05$. ROS: reactive oxygen species; DCF: dichlorodihydrofluorescein; FSC-A: forward scatter-A; SSC-A: side scatter-A.

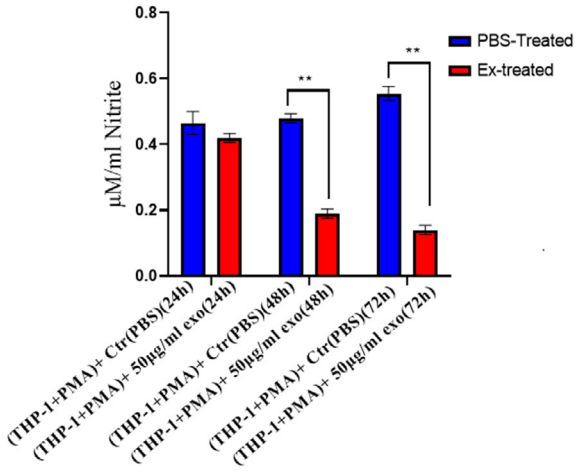

Fig. 7. Alteration of cytokine production (IL-10 and IL-6) in resting macrophages after treatment with U266-derived exosomes at 24, 48, and 72 h. The data are representative of two independent experiments presented as the mean ± SEM. **$p < 0.01$.

ROS levels were measured by the fluorescent signal of H2DCFA in M0 macrophages treated with 50 µg/mL exosomes. The findings revealed no significant changes in ROS levels within the first 24 h (13.50 ± 21.03, $p = 0.58$). However, further incubation (48 and 72 h) of M0 macrophages with exosomes induced a marginal reduction in ROS levels at 48 h (36.00 ± 10.30, $p = 0.06$) and a significant reduction in intracellular ROS levels at 72 h (117.5 ± 10.11, $P = 0.007$) compared to M0 macrophages treated with PBS (Fig. 6).

The Griess reaction was used to measure NO production at three time points, 24, 48, and 72 h. Accordingly, our results showed a reduction in NO levels at 24 h, which was not significant compared to the control group (0.045 ± 0.026, $p = 0.23$). However, as the incubation time increased, the level of NO also decreased. Therefore, the level of NO significantly decreased at 48 h (0.290 ± 0.014, $p = 0.002$) and 72 h (0.415 ± 0.018, $p = 0.001$) compared to the control group at these time points (Fig. 7).

U266B1 cell line-derived exosomes do not induce IL-6 production in M0 macrophages

IL-6 is an important factor in the pathogenesis of multiple myeloma. Accordingly, several studies have demonstrated that MM cells change the function of cells in the tumoral microenvironment to increase the mRNA and secretion of IL-6 [29]. The qRT–PCR results did not show a significant change in IL-6 mRNA levels in M0 macrophages treated with isolated exosomes compared to the control group at the defined time points (Fig. 3). Additionally, ELISA cytokine assays did not find any alteration in IL-6 protein levels in the exosome-treated group compared with their paired controls (Fig. 5).

DISCUSSION

Macrophages are a heterogeneous population of myeloid cells with remarkable polarization ability into different functional phenotypes. The main reason for the high heterogeneity of macrophages is their widespread tissue distribution, differentiation ability and responsiveness to endogenous and exogenous stimuli. Macrophages are polarized and change tissue fate in various pathophysiological events. Classically M1 and alternatively M2 activated macrophages represent two extremes of a dynamic changing state of macrophage activation. These two cell types function differently based on the type of disease. In the tumoral microenvironment, the M1 phenotype is known as tumor-resistant cells, and the M2 phenotype acts as an immune suppressor. Macrophage polarization in tumors is triggered by different stimuli, including exosomes. These nanoparticles originate from tumoral cells and deliver their contents to target cells that change their fate. Here, we investigated the effect of MM cell-derived exosomes on macrophage polarization. In this regard, a monocytic cell line (THP-1), which is frequently used to model macrophage function, was utilized in our study.

Confirmation of THP-1 differentiation was examined by changes in size/cytoplasmic volume and adherence ability, which were observed in our study. Furthermore, enhancement of granularity is another feature of M0 cells. This feature was detected by an increase in SSC on flow cytometry; moreover, Giemsa staining also manifested an obvious increase in granularity. Changes in surface markers were also assessed in our study. Previous findings in this context are inconsistent. For instance, Giovanni *et al.* [30] and Genin *et al.* [25] reported that CD14 is a monocyte marker that is downregulated during differentiation. However, in the other studies performed by Schwende *et al.* [31] and Jimenez-Duran *et al.* [32], treatment of THP-1 with PMA increased the expression of the CD14 marker. A surface marker, which almost all studies by consensus accept as a specific marker of THP-1 differentiation toward M0 cells, is CD11b, an integrin involved in cell adhesion, and we demonstrated its high expression in M0 cells. After confirmation of THP-1 differentiation into M0 cells, we found the optimum dose of MM cell-derived exosomes to

examine their effect on M0 cells. According to the study of Schwende *et al.* [31] and what we observed (arrest in the cell cycle), PMA stops cell proliferation, and therefore, no tangible difference in the number of cells was observed at different time points. However, the viability of cells was decreased at exosome doses of 75 and 100 μg/mL. Kosaka *et al.* [33] indicated that PMA caused G2 arrest. They added PMA to G2 cells, which inhibited subsequent cell division, and those growth-arrested cells did not show morphological features of mitotic cells.

Here, we demonstrated that MM cell-derived exosomes can polarize M0 cells toward M2-like cells, which show several characteristics of alternatively activated M2 macrophages. Hence, it is expected that M2-like cells function the same as M2 macrophages, including tumor-promoting capabilities involving immunosuppression, angiogenesis and neovascularization, as well as stromal activation and remodeling [21].

Polarization to the M2-like phenotype was characterized by evaluating the mRNA, specific CD marker and protein abundance of several M2 markers. Accordingly, macrophage mannose receptor (CD206) is a specific marker normally expressed on the M2 surface but not the M1 subtype and is therefore regarded as a useful marker to identify the M2 phenotype. Our findings revealed significantly increased expression of CD206 at different time points, which is in parallel with the results of Genin *et al.* [25]. M2-like cells have different profiles of cytokine secretion, including anti-inflammatory cytokines such as IL-10 [34]. Our study confirmed an increase in the mRNA and protein levels of IL-10, similar to other studies [35]. The role of IL-10 secreted by M2 macrophages is critical for tumor performance. The study by Qi *et al.* revealed that IL-10 from M2 macrophages can cooperate with JAK2 in a direct protein–protein interaction fashion, suggesting that IL-10 could form a complex with JAK2, thereby activating the JAK2/STAT3 pathway. Activation of this pathway results in the proliferation and tumorigenesis of glioma cells [36]. Arg-1, another signature of M2-like cells, is an enzyme that metabolizes l-arginine to urea and l-ornithine, limiting l-arginine bioavailability for the generation of vasoprotective NO via eNOS [37]. In fact, from a functional point of view, Arg1+ macrophages dampen T-cell activation by locally depleting L-arginine [38]. In addition, products of Arg-1 (polyamines and L-proline) play crucial roles in cell proliferation and stromal remodeling. The qRT–PCR results showed increased Arg-1 mRNA levels at different time points. Furthermore, we used the Griess assay to examine NO levels, and the results were consistent with Arg-1 mRNA levels. Although the generation of NO may be less marked in human macrophages than in rodent macrophages, a variety of conditions can stimulate NO production via NO synthase in human macrophages [39].

We also examined some specific products of M1 cells in addition to the hallmarks of M2 cells, including ROS and TNF-α. ROS are produced by all organisms, and their level in normal cells is in a dynamic but stable equilibrium balanced by the antioxidant defense system. ROS levels that exceed the capacity of the cellular antioxidant defense system induce oxidative stress [40]. In spite of participating in bacterial killing, ROS can promote antitumorigenic signaling and trigger oxidative stress–induced cancer cell death [41]. Our results showed a significant reduction in ROS levels at different time points, which can be attributed to a lack of polarization toward the M1 phenotype. This finding is in line with previous studies [12]. TNF-α plays a pivotal role in the functions of M1 cells. In the tumoral microenvironment, M1 macrophages can be stimulated to secrete a high level of TNF-α, resulting in high concentrations of superoxide, free oxygen, and nitrogen radicals, which promote cell death in the TME [42]. The qRT–PCR results showed no significant increase in TNF-α mRNA.

There is convincing evidence regarding the possible mechanism by which initial macrophage polarization in M0 cells results in M2-like cells. For instance, in the study of Lee *et al.*, miR-1305, which increased in the hypoxic TME, was suggested as a potential factor of macrophage polarization. They cocultured miR-1305-transfected RPMI 8226 cells and THP-1 macrophage cells for 48 and 72 h and observed induced expression of M2 macrophage markers in THP-1 cells [43]. The other potential mechanism is involvement of a pathway activated by IL-32. In a study by Liu *et al.*, increased levels of IL-32 in some MM cell lines (such as U266) were confirmed by RT–PCR and Western blotting [44]. Additionally, the mechanism by which IL-32 polarizes macrophages was studied by Sun *et al.* [45]. Accordingly, after confirmation of macrophage ability to phagocytose EV-IL-32, the percentage of M2 macrophages was higher, while M1 macrophages had no significant difference among each group. To confirm the role of IL-32 in macrophage polarization, the inhibitor GW4869, which can effectively inhibit the production of EVs, was used. The results showed that GW4869 significantly inhibited the secretion of EV-IL-32. Eventually, the percentage of M2 macrophages was significantly reduced when macrophages were cocultured with EVs derived from cells treated with the

inhibitor. It is well accepted that macrophage polarization is related to the activation of the STAT1 or STAT3/STAT6 signaling pathway [46]. The results of pathway evaluation demonstrated that EV-IL-32 promotes M2 macrophage polarization through phosphorylation of STAT3 [45].

Over the pathophysiology of MM, IL-6 plays an important role. This cytokine is not only a growth factor but also a survival factor and inhibitor of apoptosis for malignant plasma cells. IL-6 interacts with determinant agents in the pathogenesis of MM, such as adhesion molecules, tumor suppressor genes, and oncogenes [47]. Based on previous studies, tumor cells are able to change the function of normal resident cells into their favorable condition. Accordingly, we hypothesized that MM cell-derived exosomes might stimulate IL-6 secretion by macrophages. In line with our hypotheses, Liu *et al.* revealed that MM cell-derived exosomes from the RPMI8226 cell line promoted IL-6 secretion and osteoblastic differentiation capability of MSCs isolated from patients with MM. This finding highlights the important role of MM cell-derived exosomes in communication between tumor cells and resident cells [29]. In contrast to the study by Liu *et al.*, our results did not show the influence of MM cell-derived exosomes on the levels of IL-6 mRNA and protein. Being a pro-inflammatory cytokine, which is usually produced by M1 cells, might support this result, as MM cell-derived exosomes were effective in differentiation toward M2-like macrophages.

In spite of the strength associated with our study, some limitations should be considered: due to the presence of exosomes in commercial FBS and inaccessibility to exosome-free FBS, to resolve their interference with tumor exosomes, the FBS was ultrafiltered with AmiconUltra-15 Centrifugal Filter Units. Although this is a common procedure to deplete exosomes of FBS, many other nutrients that are essential for cells might be removed. To solve this concern, we applied an adaptation process, and no considerable alterations in the morphology of U266 cells were observed, but this might affect the quantity and quality of exosomes produced.

CONCLUSIONS

Taken together, the molecular and cellular characteristics of M0 macrophages were significantly modulated upon exposure to exosomes derived from the U266 cell line. We indicated that MM cell-derived exosomes could polarize macrophages toward M2-like cells, which promote favorable tumor functional performance. We believe that our study can be helpful in determining more about the development of leukemic niches. However, understanding the exact signaling pathway of macrophage polarization and the applicability of our findings for clinical purposes requires further studies.

The authors thank Tarbiat Modares University for its support.

FUNDING

This study was supported by Tarbiat Modares University (TMU) with grant number Med-87698.

CONFILICT OF INTEREST

The authors declare no conflict of interest.

REFERENCES

1. Cowan AJ, Green DJ, Kwok M, Lee S, Coffey DG, Holmberg LA, et al. Diagnosis and management of multiple myeloma: a review. JAMA. 2022;327(5):464–77.
2. Moreau P, Kumar SK, San Miguel J, Davies F, Zamagni E, Bahlis N, et al. Treatment of relapsed and refractory multiple myeloma: recommendations from the International Myeloma Working Group. Lancet Oncol. 2021;22(3):e105–18.
3. Hanamura I, Iida S. Multiple myeloma: update on pathophysiology and management. Rinsho Ketsueki. 2018;59(5):529–38.
4. Curado M-P, Edwards B, Shin HR, Storm H, Ferlay J, Heanue M, et al. Cancer incidence in five continents. Vol IX. Lyon: IARC Press, International Agency for Research on Cancer; 2007.
5. Sergentanis TN, Zagouri F, Tsilimidos G, Tsagianni A, Tseliou M, Dimopoulos MA, et al. Risk factors for multiple myeloma: a systematic review of meta-analyses. Clin Lymphoma Myeloma Leuk. 2015;15(10):563–77.
6. Kazandjian D. Multiple myeloma epidemiology and survival: a unique malignancy. Semin Oncol. 2016;43:676–81.
7. Fairfield H, Falank C, Avery L, Reagan MR. Multiple myeloma in the marrow: pathogenesis and treatments. Ann N Y Acad Sci. 2016;1364(1):32–51.
8. Rezaie J, Ajezi S, Avci ÇB, Karimipour M, Geranmayeh MH, Nourazarian A, et al. Exosomes and their application in biomedical field: difficulties and advantages. Mol Neurobiol. 2018;55(4):3372–93.
9. Mashouri L, Yousefi H, Aref AR, Ahadi A, Molaei F, Alahari SK. Exosomes: composition, biogenesis, and mechanisms in cancer metastasis and drug resistance. Mol Cancer. 2019;18(1):1–14.
10. Chowdhury R, Webber JP, Gurney M, Mason MD, Tabi Z, Clayton A, et al. Cancer exosomes trigger

mesenchymal stem cell differentiation into pro-angiogenic and pro-invasive myofibroblasts. Oncotarget. 2015;6(2):715.
11. Colombo M, Raposo G, Théry C. Biogenesis, secretion, and intercellular interactions of exosomes and other extracellular vesicles. Annu Rev Cell Dev Biol. 2014;30:255–89.
12. Jafarzadeh N, Safari Z, Pornour M, Amirizadeh N, Forouzandeh Moghadam M, Sadeghizadeh M. Alteration of cellular and immune-related properties of bone marrow mesenchymal stem cells and macrophages by K562 chronic myeloid leukemia cell derived exosomes. J Cell Physiol. 2019;234(4):3697–710.
13. Jafarzadeh N, Gholampour MA, Alivand MR, Kavousi S, Arzi L, Rad F, et al. CML derived exosomes promote tumor favorable functional performance in T cells. BMC Cancer. 2021;21(1):1–11.
14. Stefanovic S, Schuetz F, Sohn C, Beckhove P, Domschke C. Bone marrow microenvironment in cancer patients: immunological aspects and clinical implications. Cancer Metastasis Rev. 2013;32(1):163–78.
15. Liu J, Geng X, Hou J, Wu G. New insights into M1/M2 macrophages: key modulators in cancer progression. Cancer Cell Int. 2021;21(1):1–7.
16. Italiani P, Boraschi D. From monocytes to M1/M2 macrophages: phenotypical vs. functional differentiation. Front Immunol. 2014;5:514.
17. Mills CD, Ley K. M1 and M2 macrophages: the chicken and the egg of immunity. J Innate Immun. 2014;6(6):716–26.
18. Xiao M, Zhang J, Chen W, Chen W. M1-like tumor-associated macrophages activated by exosome-transferred THBS1 promote malignant migration in oral squamous cell carcinoma. J Exp Clin Cancer Res. 2018;37(1):1–15.
19. Shao Y, Chen T, Zheng X, Yang S, Xu K, Chen X, et al. Colorectal cancer-derived small extracellular vesicles establish an inflammatory premetastatic niche in liver metastasis. Carcinogenesis. 2018;39(11):1368–79.
20. Pinto SM, Kim H, Subbannayya Y, Giambelluca M, Bösl K, Kandasamy RK. Dose-dependent phorbol 12-myristate-13-acetate-mediated monocyte-to-macrophage differentiation induces unique proteomic signatures in THP-1 cells. bioRxiv. 2020:2020–22.
21. Genin M, Clement F, Fattaccioli A, Raes M, Michiels C. M1 and M2 macrophages derived from THP-1 cells differentially modulate the response of cancer cells to etoposide. BMC Cancer. 2015;15(1):1–14.
22. Kornilov R, Puhka M, Mannerström B, Hiidenmaa H, Peltoniemi H, Siljander P, et al. Efficient ultrafiltration-based protocol to deplete extracellular vesicles from fetal bovine serum. J Extracell Vesicles. 2018;7(1):1422674.
23. Lobb RJ, Becker M, Wen SW, Wong CS, Wiegmans AP, Leimgruber A, et al. Optimized exosome isolation protocol for cell culture supernatant and human plasma. J Extracell Vesicles. 2015;4(1):27031.
24. Shinohara H, Kuranaga Y, Kumazaki M, Sugito N, Yoshikawa Y, Takai T, et al. Regulated polarization of tumor-associated macrophages by mir-145 via colorectal cancer–derived extracellular vesicles. J Immunol. 2017;199(4):1505–15.
25. Liu Z, Liu H, Li Y, Shao Q, Chen J, Song J, et al. Multiple myeloma-derived exosomes inhibit osteoblastic differentiation and improve IL-6 secretion of BMSCs from multiple myeloma. J Investig Med. 2020;68(1):45–51.
26. Rovera G, O'Brien TG, Diamond LJS. Induction of differentiation in human promyelocytic leukemia cells by tumor promoters. Science. 1979;204(4395):868–70.
27. Schwende H, Fitzke E, Ambs P, Dieter P. Differences in the state of differentiation of THP-1 cells induced by phorbol ester and 1, 25-dihydroxyvitamin D3. J Leukoc Biol. 1996;59(4):555–61.
28. Jimenez-Duran G, Luque-Martin R, Patel M, Koppe E, Bernard S, Sharp C, et al. Pharmacological validation of targets regulating CD14 during macrophage differentiation. EBioMedicine. 2020;61:103039.
29. Mahon OR, Browe DC, Gonzalez-Fernandez T, Pitacco P, Whelan IT, Von Euw S, et al. Nano-particle mediated M2 macrophage polarization enhances bone formation and MSC osteogenesis in an IL-10 dependent manner. Biomaterials. 2020;239:119833.
30. Lian G, Chen S, Ouyang M, Li F, Chen L, Yang J. Colon cancer cell secretes EGF to promote M2 polarization of TAM through EGFR/PI3K/AKT/mTOR pathway. Biomaterials. 2019;18:1533033819849068.
31. Qi L, Yu H, Zhang Y, Zhao D, Lv P, Zhong Y, et al. IL-10 secreted by M2 macrophage promoted tumorigenesis through interaction with JAK2 in glioma. Oncotarget. 2016;7(44):71673–85.
32. Kim JH, Bugaj LJ, Oh YJ, Bivalacqua TJ, Ryoo S, Soucy KG, et al. Arginase inhibition restores NOS coupling and reverses endothelial dysfunction and vascular stiffness in old rats. J Appl Physiol. 2009;107(4):1249–57.
33. Arlauckas SP, Garren SB, Garris CS, Kohler RH, Oh J, Pittet MJ, et al. Arg1 expression defines immunosuppressive subsets of tumor-associated macrophages. Theranostics. 2018;8(21):5842–54.
34. MacMicking J, Xie QW, Nathan CJA. Nitric oxide and macrophage function. Annu Rev Immunol. 1997;15:323.
35. Herb M, Schramm MJA. Functions of ROS in macrophages and antimicrobial immunity. Antioxidants (Basel). 2021;10(2):313.
36. Forman HJ, Torres M. Redox signaling in macrophages. Mol Aspects Med. 2001;22(4–5):189–216.
37. Laha D, Grant R, Mishra P, Nilubol N. The role of tumor necrosis factor in manipulating the immunological response of tumor microenvironment. Front Immunol. 2021;12:1415.
38. Lee JY, Ryu D, Lim SW, Ryu KJ, Choi ME, Yoon SE, et al. Exosomal miR-1305 in the oncogenic activity of hypoxic multiple myeloma cells: a biomarker for predicting prognosis. J Cancer. 2021;12(10):2825.
39. Liu Y, Yan H, Gu H, Zhang E, He J, Cao W, et al. Myeloma-derived IL-32γ induced PD-L1 expression in macrophages facilitates immune escape via the PFKFB3-JAK1 axis. Oncoimmunology. 2022;11(1):2057837.
40. Sun Y, Qian Y, Chen C, Wang H, Zhou X, Zhai W, et al. Extracellular vesicle IL-32 promotes the M2 macrophage polarization and metastasis of esophageal squamous cell carcinoma via FAK/STAT3 pathway. J Exp Clin Cancer Res. 2022;41(1):1–22.

41. Sica A, Mantovani A. Macrophage plasticity and polarization: in vivo veritas. J Clin Invest. 2012;122 (3):787–95.
42. Gadó K, Domján G, Hegyesi H, Falus A. Role of interleukin-6 in the pathogenesis of multiple myeloma. Cell Biol Int. 2000;24(4):195–209.
43. Lee JY, Ryu D, Lim SW, Ryu KJ, Choi ME, Yoon SE, et al. Exosomal miR-1305 in the oncogenic activity of hypoxic multiple myeloma cells: a biomarker for predicting prognosis. J Cancer. 2021;12(10): 2825–34.
44. Liu Y, Yan H, Gu H, Zhang E, He J, Cao W, et al. Myeloma-derived IL-32γ induced PD-L1 expression in macrophages facilitates immune escape via the PFKFB3-JAK1 axis. Oncoimmunology. 2022;11(1): 2057837.
45. Sun Y, Qian Y, Chen C, Wang H, Zhou X, Zhai W, et al. Extracellular vesicle IL-32 promotes the M2 macrophage polarization and metastasis of esophageal squamous cell carcinoma via FAK/STAT3 pathway. J Exp Clin Cancer Res. 2022;41(1):1–22.
46. Sica A, Mantovani A. Macrophage plasticity and polarization: in vivo veritas. J Clin Invest. 2012;122 (3):787–95.
47. Gadó K, Domján G, Hegyesi H, Falus A. Role of interleukin-6 in the pathogenesis of multiple myeloma. Cell Biol Int. 2000;24(4):195–209.

SUPPORTING INFORMATION

Additional supporting information may be found online in the Supporting Information section at the end of the article.

Figure S1 Evaluation of the MM cell-derived exosome effect on THP-1 cells.